Acta Cryst. (1950). **3**, 379

The Determination of the Crystal Structure of Tourmaline

BY GABRIELLE DONNAY* AND M. J. BUERGER

Massachusetts Institute of Technology, Cambridge, Mass., U.S.A.

(*Received* 12 *December* 1949 *and in revised form* 24 *February* 1950)

Intensities of all accessible reflections were obtained for a Mg-tourmaline crystal from Dekalb and an Fe-tourmaline crystal from Andreasberg. Patterson–Harker sections $P(X, Y, 0)$ for each specimen were transformed to Buerger implication maps, brought to a common scale of intensities, and used together to locate the (Mg, Fe) position. The Si sites were spotted on both maps. Crystallo-chemical considerations limited the location of Al and B. The Al position was confirmed by the implication maps. Approximate sites for the anions were predicted on the basis of co-ordination and packing.

The O-tetrahedra about Si all point in the same direction; they share corners to give a ditrigonal ring. The (Mg, Fe) ion is surrounded by a slightly distorted O-octahedron, which shares two edges with adjacent octahedra and two corners with overlying tetrahedra. The Al co-ordination polyhedron is a very distorted octahedron. B lies in threefold co-ordination.

Atomic co-ordinates were refined by structure-factor calculations, which in this non-centrosymmetric case were shortened by use of the one-dimensional representation of a crystal with punched-card methods. The actual structure departs considerably from the idealized prediction.

Introduction

A description of the essential features of the crystal structure of tourmaline,

$$(Na, Ca)\,(Mg, Fe)_3B_3Al_6Si_6(O, OH, F)_{31},$$

has been briefly presented in a previous paper (Hamburger & Buerger, 1948). The purpose of the present paper is twofold: (1) to describe the method that was followed in determining the structure, particularly the use of implication mapping; (2) to give new values of the atomic co-ordinates, since the latter had to be refined when structure factors were computed for all observed $hk.l$ reflections.

Experimental procedure

A black Fe-tourmaline crystal from Andreasberg and a colorless Mg-tourmaline crystal from Dekalb were chosen for the investigation. These localities were selected because they represent simple types of tourmaline from the point of view of chemical compositions, and because reliable analyses of unusually pure crystals were available for both of them. The analyses were given in our first paper.

Both crystals used were fragments, approximately spherical in shape, 0·1–0·2 mm. in diameter. For the Dekalb Mg-tourmaline, Ni-filtered Cu K radiation was used, with $\lambda = 1{\cdot}542$ A.; for Andreasberg Fe-tourmaline, Fe-filtered Co K radiation, with $\lambda = 1{\cdot}790$ A. Dr Howard Evans read and corrected the intensities for the latter crystal. All films for intensity measurements were equi-inclination Weissenberg photographs. Films of various levels were rendered directly comparable by being given exposure times in the required ratios (Buerger & Klein, 1945). Integrated intensities were obtained by means of the Dawton technique, as perfected in this laboratory over a period of years by several investigators and described in detail by Klein (1947, pp. 14–27); the arbitrary scale of intensities ranged from 0 to 50·00. In addition, the intensities of the $hk.0$ reflections were visually estimated and recorded in decreasing order; the listing thus obtained checked the one given by the Dawton measurements. Unfortunately, many of the weak reflections (75 out of a total of 447) were not visible on the Dawton positives, although they could be seen on the original negatives.

The measured intensity $I_{hk.l}$, corrected by the Lorentz and polarization factors, as described and tabulated by Buerger & Klein (1945), yielded a value proportional to $F^2_{hk.l}$. The latter was then multiplied by 1000 in order to obtain a convenient range (0–146) of values $\sqrt{\{1000\,(1/Lp)\,I_{hk.l}\}}$ proportional to $F_{hk.l}$.

Because of the shorter wave-length used for the Mg-crystal, more reflections were obtained from it. Its data were chiefly relied on in the structure determination and were used in the comparison of observed with calculated structure factors.

Determination of structure

The cell dimensions of the Mg-tourmaline were determined with the precision Weissenberg camera. They are

$$a = 15{\cdot}95, \quad c = 7{\cdot}24\,\text{A}.$$

The space group of tourmaline (Buerger & Parrish, 1937) is $R3m$. The rhombohedral lattice is described by a hexagonal cell (Fig. 1) with additional lattice points at $\frac{2}{3}, \frac{1}{3}, \frac{1}{3}$ and $\frac{1}{3}, \frac{2}{3}, \frac{2}{3}$, so that the lattice criterion takes the form $-h+k+l=3n$. Thus the point group must be taken in the orientation $3m1$. Because of the addition of a center of symmetry by X-rays, only one-twelfth of the reciprocal-lattice points contained in the limiting sphere need to be considered, and all non-equivalent

* Arthur D. Little Fellow, Massachusetts Institute of Technology, 1948–9. Present address: Crystallographic Laboratory, The Johns Hopkins University, Baltimore 18, Md., U.S.A.

reflections can be expressed without using negative indices. The hexagonal cell contains three formula weights of composition

$$(\mathrm{Na, Ca})\,(\mathrm{Mg, Fe})_3\mathrm{B}_3\mathrm{Al}_6\mathrm{Si}_6\,(\mathrm{O, OH, F})_{31};$$

each one is associated with a lattice point and can be taken as a representative set. The equipoints are as follows:

$(0,0,0;\ \frac{2}{3},\frac{1}{3},\frac{1}{3};\ \frac{1}{3},\frac{2}{3},\frac{2}{3})+$

(3): (*a*) $0,0,z$; on three-fold rotation axis;

(9): (*b*) $2x, x, z;\ \bar{x}, x, z;\ \bar{x}, 2\bar{x}, z$; on mirror plane;

(18): (*c*) $x, y, z;\ x, x-y, z;\ \bar{y}, x-y, z;\ y-x, y, z;\ y-x, \bar{x}, z;\ \bar{y}, \bar{x}, z$; in general position.

The equipoints of the (Na, Ca) atoms alone are fixed unequivocally by space-group symmetry; they must fall on the threefold rotation axes. Because of the complexity and variation of the analyses, the ideal formula given above cannot be assumed in advance of the solution of the structure. Therefore the equipoint locations of all other atoms are uncertain. In the following discussion we shall consider only the atoms of the representative set about the origin.

Two Patterson–Harker syntheses $P(X, Y, 0)$ were performed: one with the Dekalb data, the other with the Andreasberg data. The results for the Dekalb crystal are shown in Fig. 2. The syntheses were then transformed into implication diagrams $I3(x, y, 0)$ (Figs. 3, 4) by rotating the co-ordinate axes through 30° and multiplying by the shrinkage factor $(\sqrt{3})/3$ (Buerger, 1946), as illustrated in Fig. 5. The centrosymmetric ambiguity and the satellites that result, in point group $3m$, from atoms in equipoints (*b*), equipoints (*c*) with $y=0$, and equipoints (*c*) with $y\neq 0$, are shown in Fig. 6.

On both implication diagrams (Figs. 3, 4), the second of these three possibilities, equipoints (*c*) with $y=0$, is immediately recognized, because the six strongest peaks around the trace of a threefold rotation axis lie half-way between the mirror planes, and their satellites lie on the mirror planes. For the Mg-tourmaline crystal, the strongest peaks are expected to be Si peaks, since the silicon atoms are the densest atoms in this structure. The Si atoms were, therefore, tentatively placed on these peaks. Their position ($x=0{\cdot}19, y=0$) is centrosymmetric in the xy projection. In order to simplify the calculations, we assumed, as a first guess, that the signs of $F_{hk.0}$ structure factors were controlled by the atoms at $x=0{\cdot}19, y=0$. An electron-density projection on (00.1) was evaluated (Fig. 7). The highest peak occurs on the position at which the atom was placed. The second highest peak is found on the mirror plane, in site (*b*) with $x=0{\cdot}067$. This position happens to coincide with one group of satellites of the strongest peak on the implication diagram, a circumstance which masks the fact that it represents the first possibility of Fig. 6. It was interpreted as a likely site for (Mg, Fe) atoms.

The presence of isomorphous replacement enabled us to check the above hypothesis. The two specimens used in the analysis mainly differ in that the Fe of one is replaced by Mg in the other. If the data for both crystals had been obtained on the absolute scale or on the same arbitrary scale, the 'difference implication' could be computed. (This function gives at any point the difference between the implications $I3(x, y, 0)$ for Fe and Mg tourmalines.) On such a map the only peak expected to occur, with its ambiguity and satellites of course, would represent the (Mg, Fe) position. A similar procedure was suggested for F^2 summations by the senior author (Buerger, 1942). The conversion factor necessary to bring the two implications to the same scale is obtained in the following way: Assume that the bottom of the lowest depression near the origin on the two implication maps is the true zero level. Its depth, in absolute value, is then proportional to $F^2_{00.0}=(\sum_n f_n)^2$. Write that k times the observed minimum is equal to $(\sum_n f_n)^2$, and determine the k values for both crystals:

	Andreasberg (Fe)	Dekalb (Mg)
Observed minimum	1398	354
$(\sum_n f_n)^2$	510^2	487^2
k	186	670

The conversion factor, by which the Andreasberg implication function must be multiplied in order to be brought to the same scale as the Dekalb implication function, is given by the ratio of the corresponding k's, namely $186/670=0{\cdot}277$.

Accordingly, to form the difference implication, the Andreasberg implication function was multiplied by 0·277, and the Dekalb implication function subtracted from it. The result (Fig. 8) shows that the outstanding peak does coincide with the second highest peak of the electron-density projection (ignoring the origin peak); the tentative placement of (Fe, Mg) on the 9 (*b*) equipoint with $x=0{\cdot}067$ is thus confirmed.

A comparison of the volumes under the Si and Mg peaks on the Dekalb implication map made us suspect that more than one Si–Si interaction must contribute to the Si peak, assuming that the latter receives no non-Harker contribution. In an attempt to resolve the peak we performed a 'sharpened' F^2 summation, ${}_sP(X, Y, 0)$. The procedure used is a modification of that suggested by Patterson (1935). F^2 terms are corrected to the value they would have if atoms were reduced to points. An averaged normalized f_n curve is obtained by plotting $\sum_n f_n/\sum_n Z_n$, where Z_n is the atomic number of the nth atom. The summation ${}_sP(X, Y, 0)$ is defined as

$${}_sP(X, Y, 0)=\sum_{h=-\infty}^{\infty}\sum_{k=-\infty}^{\infty}\left[\sum_{l=-\infty}^{\infty}F^2_{hkl}\left(\frac{\sum_n Z_n}{\sum_n f_n}\right)^2\right]\cos 2\pi(hx+ky).$$

Although the maxima are sharper, the Si peak in question is not resolved (Fig. 9). This led us to believe that an atom must be almost exactly above Si.

To obtain more decisive evidence, a Patterson section $P(X,0,Z)$ was computed (Fig. 10). A peak appears at $X=0$, $Z=1{\cdot}6$ A. The corresponding interatomic vector is vertical and its length, 1·6 A., is the usual Si–O distance. When an oxygen (which we shall call the 'apical oxygen' for convenience) is placed directly below the silicon, the three oxygens needed to complete the co-ordination tetrahedron are expected to lie in a plane parallel to (00.1). The oxygens closest to the origin must lie on mirror planes because the oxygen radius is too large to permit placing them between mirrors. These oxygens are shared by adjacent tetrahedra, thus forming a six-membered ring of tetrahedra. The observed Si–Si distance of 3·06 A. is a reasonable one for this configuration. The latter also provides oxygen linkages between Si and Mg co-ordination polyhedra, to be discussed below, and this further strengthens the ring hypothesis.

We have seen that three magnesiums form a horizontal equilateral triangle. We expect magnesium to be octahedrally surrounded by oxygens. The Mg–Mg distance is so small (about 3 A.) that each Mg co-ordination octahedron must share an inclined edge with each of its two neighbors (Fig. 13). The lower faces of the octahedra form a ring of three triangles, each of which has two of its corners shared with its neighbors, while the third corner, unshared, is occupied by an OH group. The upper faces of the octahedra share a single corner, an OH, which lies on the threefold rotation axis, while the other two corners are occupied by the apical oxygens of two Si tetrahedra in the ring above. The three layers of oxygens roughly account for the measured cell height. At this point in the structure determination we had accounted for most of the atoms in the tourmaline formula. Still to be located were six aluminums, six oxygens and three borons (for one third of the hexagonal cell only).

Space-group symmetry requires the aluminum to go either in one sixfold position or in two threefold positions on the mirror planes. Since the implication maps did not show any sharp peak not already accounted for as atomic position, satellite or ambiguity, we had at first placed the aluminums on the same peaks as the Si atoms. This led us to consider a double ring of tetrahedra, six of them with Si at their centers and six more above these with Al at their centers.* A very objectionable consequence of this structure was that Al was no longer available to tie the three structural islands together. Also a fourfold co-ordination of Al in tourmaline was surprising since Al is known (from chemical analyses in the literature) to be partly replaced by Mg, which, in all known cases but one, is in octahedral co-ordination. Furthermore, Pauling's Electrostatic Valence Rule was not satisfied by this structure. For these crystallo-chemical reasons, the double-ring structure was abandoned.

There are usually several ways of interpreting collections of peaks in any map. An alternate structure is suggested by the implication maps, which show maxima coalescing into a ring around the 3_1 axis. Aluminum, if placed on this ring, is in a general (sixfold) position. Each of the structural units contributes one of its six aluminums to the ring, so that these aluminums will lie on a helix about the 3_1 axis. They are placed in such a way that each of them has four oxygens as nearest neighbors. Two of these oxygens are part of one structural unit, each of the other two is part of another. At this juncture it became apparent that, by placing the remaining six oxygens in a general position, we could complete an octahedron about each aluminum and at the same time create roughly equilateral triangles into which the three borons could be placed. Pauling's Electrostatic Valence Rule now was rigorously satisfied for all oxygens and OH groups, except that the apical oxygen receives bond strength $1\frac{5}{6}$ instead of 2 and the OH in threefold position $1\frac{1}{3}$ instead of 1.

The resulting arrangement satisfied all structural requirements and showed satisfactory agreement between calculated and observed structure factors for all three axial zones; it ultimately proved to be the correct one. We proceeded to determine the atomic parameters more accurately.

Refinement of parameters

From the implication map we knew the x and y parameters of Si and Mg with fair accuracy and those of Al approximately. We had, however, no reliable information concerning the oxygen sites. Our first move was to make the co-ordination polyhedra as close to regular solids as possible, starting with the tetrahedra and proceeding with the octahedra, first around Mg, then around Al. The ring of tetrahedra acquired hexagonal symmetry ($6mm$), the Mg octahedra could be made regular, but the Al octahedra always remained somewhat irregular. This idealized structure was ruled out at once by the lack of agreement between observed and calculated $hk.0$ structure factors.

We proceeded to vary x and y parameters until reasonably good agreement was reached. It appeared at this point that the method of successive approximations by means of electron-density projections might be profitably applied. The results were disappointing. In every case, the projection returned to us the atomic sites which we had assumed for phase calculations, even when these sites, as it turned out later, were considerably in error. The failure of the method can probably be accounted for as follows: In a non-centrosymmetric structure the magnitude of the Fourier coefficients A and B depends on the atomic co-ordinates. Therefore, an error is made in every term, whereas in a centrosymmetric structure errors are introduced only for those terms for which the wrong sign is used. When the para-

* This structure was tentatively suggested in our report at the Yale meeting of the Crystallographic Society of America, 1 April 1948. The printed abstract, however, gave the correct structure.

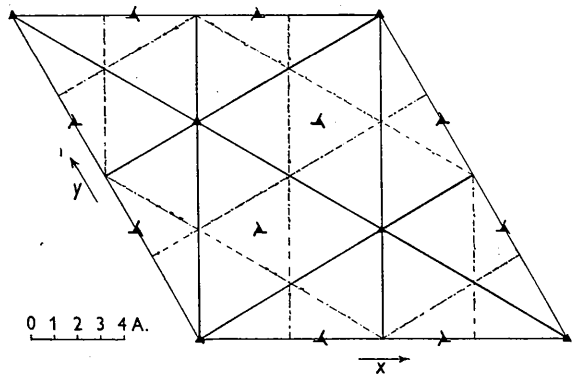

Fig. 1. Space group of tourmaline projected on (00.1).

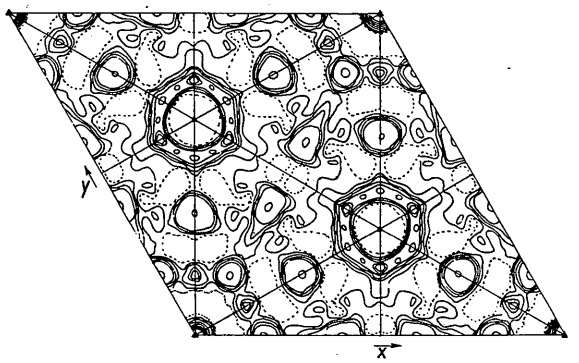

Fig. 2. Patterson–Harker section $P(X, Y, 0)$ for Mg-tourmaline. Positive-contour interval is 100 on arbitrary scale. It is the same on all diagrams.

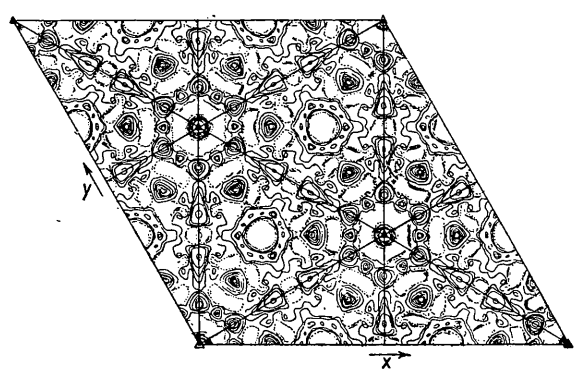

Fig. 3. Implication diagram $I3(x, y, 0)$ for Mg-tourmaline.

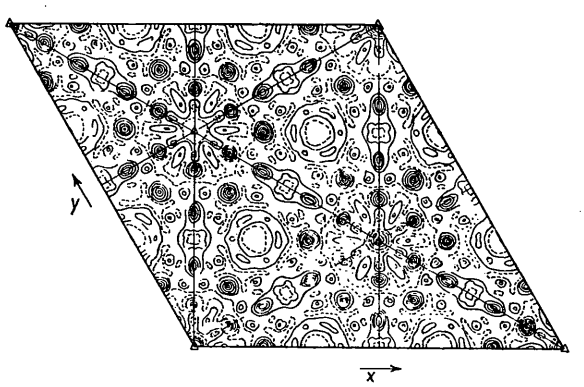

Fig. 4. Implication diagram $I3(x, y, 0)$ for Fe-tourmaline.

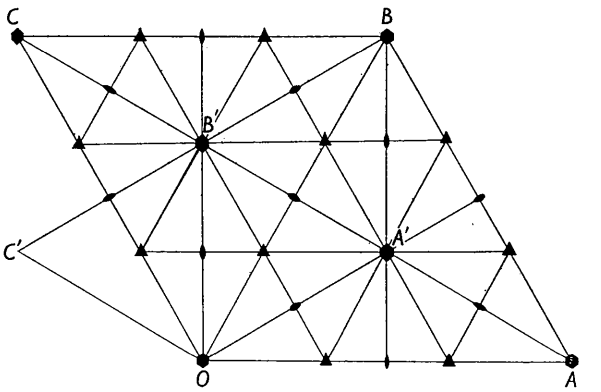

Fig. 5. Transformation of unit cell from Patterson space to implication space. The section $OABC$ through the cell in Patterson space is transformed to the rhomb $OA'B'C'$ in implication space. The symmetry elements of the crystal cell as shown in Fig. 1 operate on $OA'B'C'$ to give the projection $OABC$ of a unit cell in implication space. The symmetry elements shown are those of the projected cell in implication space.

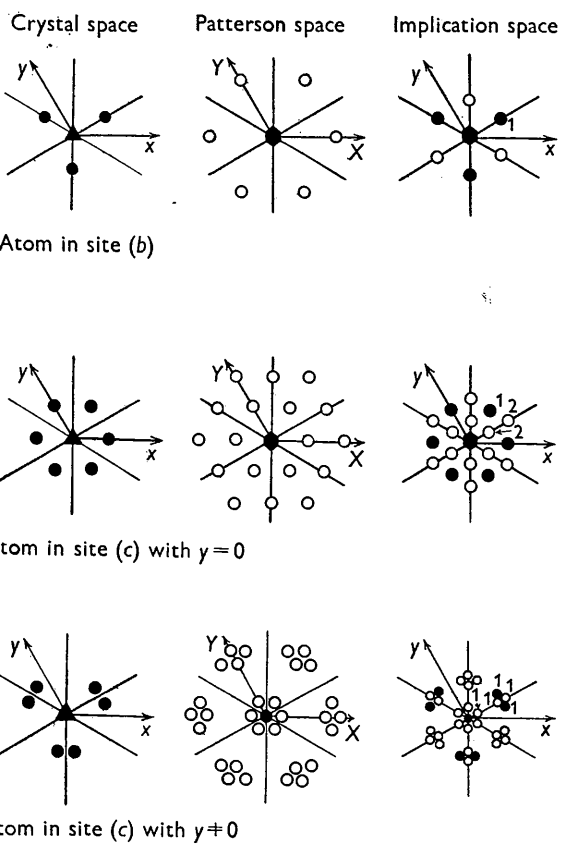

Fig. 6. Transformation of one atomic site from crystal space to Patterson space and to implication space for point group $3m$. In implication space the black dots are the atomic sites. The numbers give the weights of the peaks.

meters are close to the true ones, only a few small terms usually are in error. It appears, therefore, that for non-centrosymmetric structures one should not depend too much on electron-density summations. We relied on structure-factor agreement and succeeded in reducing the 'discrepancy index'

$$\Sigma \,|\, |F_{\text{obs.}}| - |F_{\text{calc.}}| \,| \div \Sigma |F_{\text{obs.}}|$$

to 0·18 (for $hk.0$ reflections only).

was then put to the test of structure-factor calculations for all reflections. The need for further refining of parameters became apparent. Inasmuch as the usual method of computing structure factors by means of the simplified trigonometric expansion was very slow—about four hours for one $hk.l$—, the graphical method (Donnay, 1949) based on the one-dimensional representation of the crystal was used during the first part of these calculations. In view of the large number of reflections,

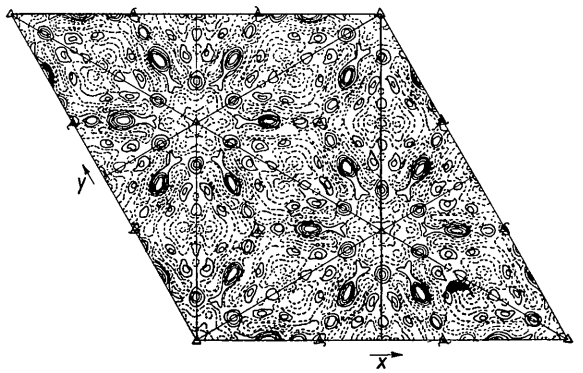

Fig. 7. Electron-density projection on (00.1) for Fe-tourmaline. Signs of F_{hk0}'s are controlled by atom at $x=0{\cdot}19$, $y=0$.

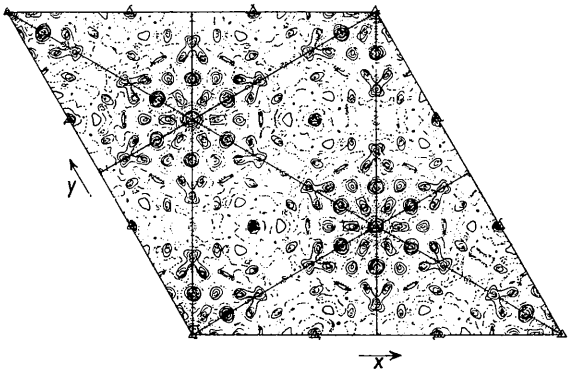

Fig. 8. Difference implication diagram.
$I3(x, y, 0)$ Fe-tourmaline $-$ $I3(x, y, 0)$ Mg-tourmaline.

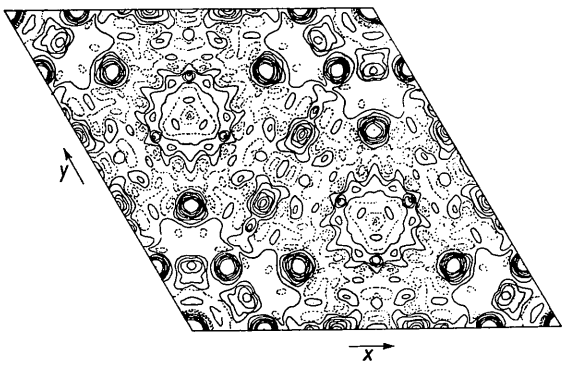

Fig. 9. 'Sharpened' Patterson–Harker section ${}_sP(X, Y, 0)$ for Mg-tourmaline.

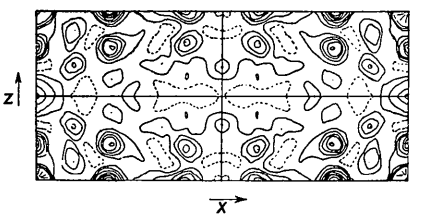

Fig. 10. Patterson section $P(X, 0, Z)$ for Mg-tourmaline.

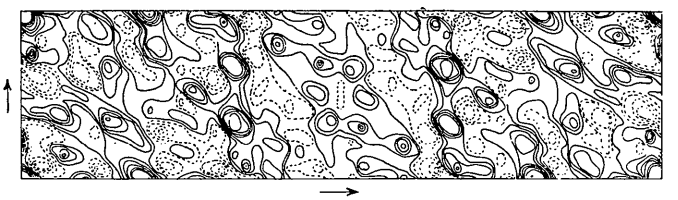

Fig. 11. Patterson section $P(X', 0, Z)$ parallel to (21.0) for Mg-tourmaline.

The z parameters were modified from what they were in the idealized structure by making use of the information yielded by two vertical sections through Patterson space, namely $P(X, 0, Z)$, already mentioned (Fig. 10), and $P(X', 0, Z)$ parallel to (21.0) (Fig. 11). For oxygens and borons consideration of interatomic distances was found helpful. The discrepancy index for $h0.l$ and $0k.l$ reflections was found to be 0·28.

The structure thus found from axial-zone data only however, it became imperative to resort to digital calculators in order to accelerate the computations even more. At first we tried to limit changes in co-ordinates to the z parameters. However, a large number of such attempts proved futile. Reluctantly we also had to modify some x and y parameters even though it increased the discrepancy index of $hk.0$ reflections. A good many more trials finally led to the parameters listed in Table 1. The co-ordinates of the metal atoms are

Table 1. *Co-ordinates of the atoms in tourmaline of composition* (Na, Ca)$Mg_3B_3Al_6Si_6O_{27}(OH)_4$

Atom	Position	x	y	z
Na, Ca	3 (*a*)	0	0	0·786
Mg	9 (*b*)	0·134	0·067	0·154
B	9 (*b*)	0·117	0·234	0
Al	18 (*c*)	0·065	0·365	0·834
Si	18 (*c*)	0·192	0·192	0·522
O_1=OH	3 (*a*)	0	0	0·315
O_2	9 (*b*)	0·058	0·116	0
O_3=OH	9 (*b*)	0·234	0·117	0·938
O_4	9 (*b*)	0·096	0·192	0·593
O_5	9 (*b*)	0·160	0·080	0·522
O_6	18 (*c*)	0·196	0·196	0·315
O_7	18 (*c*)	0·275	0·255	0·671
O_8	18 (*c*)	0·050	0·286	0

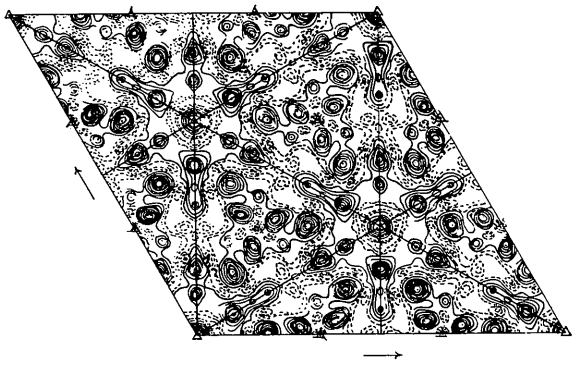

Fig. 12. Electron-density projection on (00.1) for Mg-tourmaline.

presumably accurate to ±0·01 A., those of the oxygen atoms to ±0·02 A. These parameters were used for calculating the structure factors which are compared with the observed values in Table 2.

The discrepancy index was computed in two different ways: (1) All non-equivalent reflections were given the same weight, regardless of multiplicity. (2) Non-equivalent reflections were given weights equal to their

Table 2. *Metal–oxygen distances*

Metal	No. of oxygens	Oxygen designation	Distance (A.)
Si	1	O_4	1·60
	1	O_5	1·60
	1	O_6	1·50
	1	O_7	1·56
B	1	O_2	1·59
	2	O_8	1·59
Al	1	O_3	2·67
	1	O_6	1·78
	1	O_7	1·98
	1	O_7*	2·25
	1	O_8	1·65
	1	O_8†	1·65
Mg	1	O_1=OH	2·16
	2	O_2	2·08
	1	O_3=OH	2·12
	2	O_6	2·10
Na, Ca	1	O_1	2·28
	3	O_2	2·22

* Atom O_7 in the 'molecule' about lattice point $\frac{2}{3}, \frac{1}{3}, \frac{1}{3}$.
† Atom O_8 in the 'molecule' about lattice point $\frac{1}{3}, \frac{2}{3}, \frac{2}{3}$.

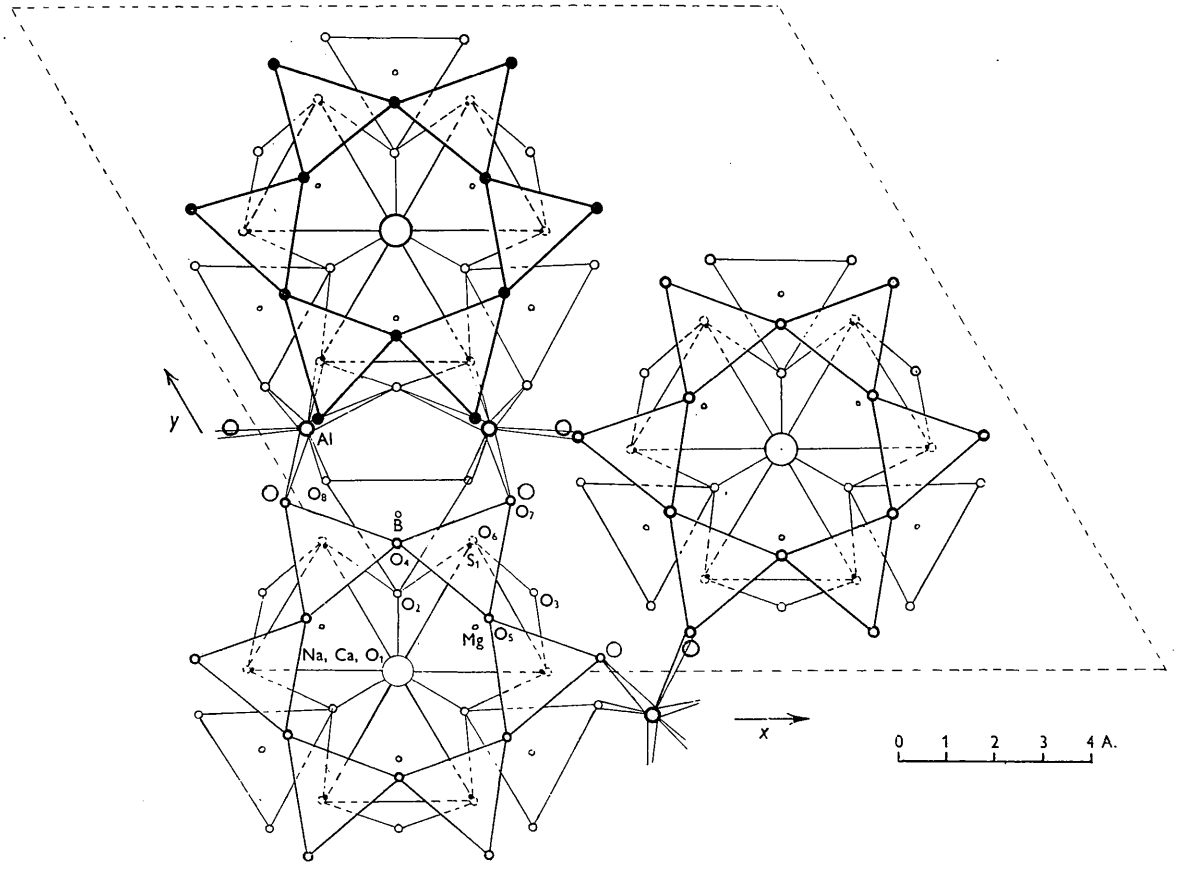

Fig. 13. Crystal structure projected on (00.1) and seen from above. Atoms are labelled as shown in Table 1.

multiplicity; this amounted to giving the same weight to all accessible reciprocal-lattice points. The results were 0·37 and 0·36, respectively. Thus in the present case there is no need to use the second method. The agreement still leaves much to be desired.

The high value of the index is unquestionably due, to some extent, to the preponderance of small observed structure factors (Abrahams & Robertson, 1949). Moreover, for a non-centrosymmetric structure one cannot expect the discrepancy index to be as low as for a centrosymmetric one, for similar departures from the true parameters. Additional unfavorable circumstances which account in part for the high value of the index are: (1) the complexity of the chemical composition with its large range of solid solutions, which led us to assume an idealized formula; (2) the lack of absorption and extinction corrections. In view of these considerations and of the length of the calculations, we feel that we have reached the point of diminishing returns.

The description of the structure given in our previous paper remains unchanged. (As this paper appears in proof, a different structure for tourmaline is reported (Belov & Belova, 1949).) Our results agree roughly with those of Sadanaga (1948), whose abstract has only recently come to our attention. The final electron-density projection $p(x,y,0)$ (Fig. 12) and a revised drawing (Fig. 13) are given here. The new metal–oxygen distances are shown in Table 2.

The junior author (G.D.) wishes to express her gratitude to Prof. B. E. Warren of the Massachusetts Institute of Technology for his helpful advice and encouragement. She is also indebted to Dr L. H. Thomas, of the Watson Scientific Computing Laboratory at Columbia University, for permission to use the I.B.M. equipment, and to other members of the staff of the Laboratory for their courtesy and assistance.

References

Abrahams, S. C. & Robertson, J. M. (1949). *Acta Cryst.* **1**, 252.

Belov, N. V. & Belova, E. N. (1949). *Dokl. Akad. Nauk, S.S.S.R.* **69** (no. 2), 185 (abstracted in *Physics Abstracts* (1950), **53**, p. 431, item 3545).

Buerger, M. J. (1942). *Proc. Nat. Acad. Sci., Wash.*, **28**, 281.

Buerger, M. J. (1946). *J. Appl. Phys.* **17**, 579.

Buerger, M. J. & Klein, G. E. (1945). *J. Appl. Phys.* **16**, 408.

Buerger, M. J. & Parrish, William (1937). *Amer. Min.* **22**, 1139.

Donnay, Gabrielle H. (1949). *Acta Cryst.* **2**, 370.

Hamburger, Gabrielle E. & Buerger, M. J. (1948). *Amer. Min.* **33**, 532.

Klein, G. E. (1947). The Crystal Structure of Nepheline. Master's Thesis, Massachusetts Institute of Technology.

Patterson, A. L. (1935). *Z. Krystallogr.* **90**, 517.

Sadanaga, R. (1948). *J. Geol. Soc. Tokyo*, **53**, 52.

Table 3. *Comparison of observed and calculated structure factors*

Reflection	sin θ	$A_{calc.}$	$B_{calc.}$	$\lvert F_{calc.}\rvert$	$F_{obs.}$	Reflection	sin θ	$A_{calc.}$	$B_{calc.}$	$\lvert F_{calc.}\rvert$	$F_{obs.}$
00.3	0·320	−19·42	−55·10	58	76	12.0..6	0·925	−12·77	22·80	26	36
00.6	0·645	130·84	5·24	131	87	13.0..1	0·730	7·41	9·23	12	14
00.9	0·965	−10·85	−25·44	28	37	13.0..4	0·840	−17·17	−12·99	21	*w*
10.1	0·120	−15·06	−16·26	22	10	14.0..2	0·805	−19·72	11·71	23	10
10.4	0·430	24·89	−24·55	35	32	14.0..5	0·945	15·19	1·54	15	26
10.7	0·750	6·59	1·48	7	17	15.0..0	0·835	45·40	− 9·16	46	50
20.2	0·240	− 5·44	− 6·80	9	*w*	15.0..3	0·895	−14·32	5·63	15	24
20.5	0·545	− 8·15	−15·02	17	14	16.0..1	0·895	− 8·24	3·41	9	*w*
20.8	0·865	17·20	−13·47	22	17						
30.0	0·165	38·78	−14·55	42	41	01.2	0·220	37·99	−23·94	47	58
30.3	0·360	− 6·87	−61·95	62	36	01.5	0·540	− 2·77	59·39	60	52
30.6	0·665	26·58	14·37	30	33	01.8	0·860	0·77	−34·65	35	30
30.9	0·980	0·27	−23·18	23	14	11.0	0·095	− 0·06	0	0	0
40.1	0·245	15·64	− 2·68	16	17	11.3	0·335	−11·61	− 6·02	13	10
40.4	0·485	− 3·36	1·74	4	36	11.6	0·650	−15·20	12·59	20	10
40.7	0·780	− 6·87	− 1·99	7	17	11.9	0·970	7·00	− 3·66	8	14
50.2	0·350	65·07	− 3·11	65	47	21.1	0·180	36·88	8·63	38	45
50.5	0·605	−89·39	8·07	90	123	21.4	0·455	−24·23	− 8·01	25	*w*
50.8	0·900	30·32	−28·58	42	14	21.7	0·765	− 1·82	−16·81	17	17
60.0	0·335	10·42	−17·89	21	28	31.2	0·295	−47·53	6·78	48	20
60.3	0·465	−29·78	−47·30	56	50	31.5	0·570	9·75	−18·97	21	10
60.6	0·725	5·79	7·20	9	20	31.8	0·880	− 3·22	− 7·98	9	14
70.1	0·405	4·38	−12·28	13	17	41.0	0·255	36·54	−10·67	39	41
70.4	0·580	− 4·88	8·89	10	17	41.3	0·410	16·33	−18·92	25	*w*
70.7	0·845	− 2·53	− 0·81	3	17	41.6	0·690	6·20	9·72	12	*w*
80.2	0·495	− 8·89	7·05	11	20	51.1	0·330	−45·18	−18·00	49	55
80.5	0·695	3·51	− 0·03	4	22	51.4	0·530	23·69	−87·10	90	92
80.8	0·965	−13·08	− 0·79	13	*w*	51.7	0·810	−21·25	22·94	31	30
90.0	0·500	− 1·37	−19·31	19	57	61.2	0·420	− 8·42	− 7·08	11	14
90.3	0·595	17·01	1·14	17	20	61.5	0·650	0·34	4·45	4	17
90.6	0·815	−21·41	23·40	32	30	61.8	0·930	− 9·12	−11·57	15	17
10.0..1	0·565	−90·22	−11·11	91	116	71.0	0·420	− 7·52	16·87	19	10
10.0..4	0·700	28·80	−50·45	58	57	71.3	0·530	12·50	0·28	13	14
10.0..7	0·935	−34·54	− 8·37	35	10	71.6	0·770	− 9·97	− 3·63	11	*w*
11.0..2	0·650	−13·16	16·62	21	*w*	81.1	0·485	17·77	30·35	35	22
11.0..5	0·810	−27·54	18·93	33	24	81.4	0·640	− 0·74	− 6·28	6	17
12.0..0	0·665	− 6·98	−39·07	40	17	81.7	0·890	− 1·82	1·41	2	10
12.0..3	0·740	− 9·18	− 7·53	12	*w*	91.2	0·570	− 2·21	10·15	10	14

Table 3 (*cont.*)

Reflection	sin θ	$A_{calc.}$	$B_{calc.}$	$\lvert F_{calc.} \rvert$	$F_{obs.}$
91.5	0·755	8·50	12·67	15	14
10.1..0	0·585	57·67	25·80	64	83
10.1..3	0·670	−24·92	46·00	52	54
10.1..6	0·870	20·99	−26·30	34	20
11.1..1	0·650	−35·23	26·10	44	32
11.1..4	0·770	14·99	− 5·12	16	14
12.1..2	0·730	− 7·46	0·76	8	17
12.1..5	0·880	2·68	4·57	5	14
13.1..0	0·750	6·78	11·70	14	*w*
13.1..3	0·815	− 4·88	− 3·37	6	*w*
14.1..1	0·815	− 7·85	− 7·70	11	10
14.1..4	0·915	11·20	4·90	12	14
15.1..2	0·890	5·70	− 6·70	9	10
16.1..0	0·920	36·43	−10·55	38	30
16.1..3	0·970	−15·57	− 5·88	17	10
02.1	0·155	− 5·92	5·91	8	32
02.4	0·445	26·45	− 1·54	27	20
02.7	0·760	− 4·95	6·38	8	22
12.2	0·260	−33·22	26·03	42	75
12.5	0·555	3·30	− 2·49	33	*w*
12.8	0·870	− 8·99	17·30	20	14
22.0	0·190	−75·43	0	75	94
22.3	0·375	21·29	−22·65	31	47
22.6	0·670	−36·39	19·45	41	17
32.1	0·265	11·08	36·67	38	22
32.4	0·490	18·51	− 4·36	19	22
32.7	0·790	−21·75	1·06	22	20
42.2	0·365	−16·49	46·64	50	37
42.5	0·610	5·08	3·44	6	*w*
42.8	0·905	− 9·09	19·18	21	*w*
52.0	0·345	9·74	− 3·39	10	10
52.3	0·475	− 9·89	−12·44	16	*w*
52.6	0·730	− 9·76	4·01	11	10
62.1	0·415	20·27	10·89	23	41
62.4	0·585	1·92	− 7·87	8	20
62.7	0·850	1·55	−13·37	13	10
72.2	0·505	−56·66	28·42	64	47
72.5	0·700	37·13	−18·63	42	22
72.8	0·970	−14·65	12·78	19	10
82.0	0·510	− 4·91	35·94	36	35
82.3	0·600	2·11	5·88	6	10
82.6	0·820	− 0·08	0·31	0	*w*
92.1	0·575	5·99	− 2·75	7	10
92.4	0·710	19·66	13·81	24	*w*
92.7	0·940	− 0·20	− 7·25	7	*w*
10.2..2	0·655	−12·98	20·87	25	14
10.2..5	0·820	18·87	− 0·87	19	10
11.2..0	0·675	− 2·62	13·59	14	10
11.2..3	0·745	− 5·34	− 3·76	7	*w*
11.2..6	0·930	− 8·28	− 4·66	9	*w*
12.2..1	0·735	38·83	− 6·78	40	24
12.2..4	0·845	− 6·97	24·06	25	17
13.2..2	0·815	−19·28	−12·76	23	14
13.2..5	0·950	15·55	18·34	18	10
14.2..0	0·840	15·82	8·79	16	0
14.2..3	0·900	− 7·82	−12·54	15	14
15.2..1	0·900	4·90	−14·33	15	*w*
03.3	0·360	− 5·27	2·72	6	33
03.6	0·665	31·41	4·74	32	26
03.9	0·980	3·30	5·96	7	*w*
13.1	0·225	24·99	− 1·94	25	22
13.4	0·475	0·28	10·77	11	10
13.7	0·775	9·57	− 2·11	10	0
23.2	0·325	12·71	26·44	29	32
23.5	0·590	6·78	− 7·87	10	22
23.8	0·890	1·88	8·21	8	17
33.0	0·290	3·72	0	4	10
33.3	0·430	− 1·27	4·24	4	22
33.6	0·705	−23·45	20·39	31	30
43.1	0·355	28·36	21·97	36	52
43.4	0·545	−26·72	35·81	45	69
43.7	0·825	10·26	−16·62	20	39
53.2	0·445	6·53	−29·13	30	10
53.5	0·660	− 5·89	− 4·50	7	*w*
53.8	0·940	16·17	−18·67	25	26
63.0	0·440	−13·50	−11·19	17	*w*
63.3	0·545	−12·77	−37·31	40	40
63.6	0·780	−11·39	15·52	19	10
73.1	0·505	10·62	−13·00	17	14
73.4	0·655	− 7·71	20·48	22	10
73.7	0·900	− 8·85	−19·29	21	30
83.2	0·590	−35·00	3·41	35	33
83.5	0·765	16·55	− 3·52	17	10
93.0	0·600	−42·02	−37·89	57	41
93.3	0·680	30·21?	−39·88	50	35
93.6	0·880	−16·79	44·75	48	33
10.3..1	0·665	13·44	1·36	14	28
10.3..4	0·785	3·20	15·03	15	*w*
11.3..2	0·740	−11·23	22·19	25	14
11.3..5	0·890	3·58	0·20	4	17
12.3..0	0·765	1·39	−20·00	20	*w*
12.3..3	0·830	11·23	−16·95	20	20
13.3..1	0·825	18·51	23·10	30	22
13.3..4	0·925	−20·98	−18·87	28	10
14.3..2	0·900	−26·05	4·77	27	17
15.3..0	0·930	−11·01	16·46	20	20
04.2	0·310	−43·10	−17·20	46	17
04.5	0·580	14·99	31·38	35	57
04.8	0·885	−33·54	−30·74	45	17
14.3	0·410	1·60	31·36	31	20
14.6	0·690	6·68	−14·86	16	17
24.1	0·315	−10·00	11·34	15	14
24.4	0·520	−12·32	−34·59	37	30
24.7	0·805	− 6·10	− 5·57	8	*w*
34.2	0·400	−27·60	−48·16	56	96
34.5	0·635	40·95	7·63	42	32
34.8	0·920	−14·63	−11·39	19	35
44.0	0·385	55·85	0	56	50
44.3	0·500	− 1·53	− 6·21	6	*w*
44.6	0·750	12·79	11·57	17	28
54.1	0·445	−18·84	− 1·84	19	10
54.4	0·610	−14·97	−55·85	58	42
54.7	0·865	− 0·54	3·63	4	*w*
64.2	0·530	11·81	−29·71	32	40
64.5	0·720	−19·89	26·74	33	26
74.0	0·535	42·38	8·40	43	42
74.3	0·625	− 2·18	− 2·81	4	14
74.6	0·835	28·29	11·89	31	10
84.1	0·600	29·02	32·71	44	30
84.4	0·730	−18·89	5·57	20	*w*
84.7	0·955	− 0·15	14·18	14	10
94.2	0·675	14·94	9·10	18	17
94.5	0·835	− 5·65	−11·48	13	22
10.4..0	0·695	10·40	−16·29	19	10
10.4..3	0·765	− 3·98	1·96	4	0
10.4..6	0·945	− 2·22	4·11	5	10
11.4..1	0·755	−23·58	27·36	36	28
11.4..4	0·860	20·46	−29·71	36	35
12.4..2	0·836	19·87	− 0·52	20	20
12.4..5	0·965	−20·52	11·53	24	39
13.4..0	0·855	−17·94	1·08	18	*w*
13.4..3	0·915	5·19	4·97	7	10
14.4..1	0·915	−14·04	8·15	16	14
05.1	0·300	−134·15	24·88	137	146
05.4	0·510	78·49	−39·77	88	115
05.7	0·800	−53·20	15·69	55	20
15.2	0·375	−30·94	69·27	76	92
15.5	0·620	−21·66	13·99	26	22
15.8	0·910	−13·95	− 3·44	14	28
25.3	0·475	− 5·10	1·71	5	0
25.6	0·730	− 0·72	12·53	13	17
35.1	0·405	−13·03	2·54	13	10
35.4	0·580	24·14	16·06	29	28
35.7	0·845	− 6·25	− 1·52	6	24
45.2	0·485	−18·23	29·90	35	28
45.5	0·690	− 5·20	26·26	27	10
45.8	0·960	−11·52	1·54	12	35
55.0	0·480	117·95	0	118	139

Table 3. (*cont.*)

Reflection	sin θ	$A_{calc.}$	$B_{calc.}$	$\lvert F_{calc.}\rvert$	$F_{obs.}$
55.3	0·580	−53·38	16·38	56	37
55.6	0·805	53·15	− 4·05	53	45
65.1	0·540	0·84	−29·65	30	41
65.4	0·680	40·68	− 2·60	41	26
65.7	0·920	− 3·59	2·65	4	24
75.2	0·620	−15·52	24·40	29	20
75.5	0·790	12·57	− 8·35	15	24
85.0	0·630	−17·27	− 3·16	17	17
85.3	0·710	− 3·75	−24·54	25	*w*
85.6	0·900	−16·04	9·31	19	10
95.1	0·690	5·12	−22·31	23	20
95.4	0·805	− 4·76	−16·81	17	10
10.5..2	0·765	18·36	6·90	20	10
10.5..5	0·910	−29·15	14·15	33	59
11.5..0	0·785	31·26	8·20	32	22
11.5..3	0·850	− 8·93	− 3·30	10	*w*
12.5..1	0·850	2·15	−11·94	12	10
12.5..4	0·945	− 7·84	−12·43	15	14
13.5..2	0·920	−25·58	−12·82	29	20
06.3	0·465	−40·95	57·21	70	100
06.6	0·725	5·98	−28·97	30	39
16.1	0·380	− 5·34	16·35	17	30
16.4	0·560	− 0·70	6·94	7	0
16.7	0·835	−11·52	− 5·36	13	10
26.2	0·455	− 1·49	7·19	7	24
26.5	0·670	25·25	− 4·34	25	*w*
26.8	0·945	10·03	9·67	14	17
36.3	0·545	− 8·19	6·60	11	17
36.6	0·780	− 8·49	6·31	11	*w*
46.1	0·495	−15·30	−21·86	27	32
46.4	0·645	35·76	− 2·16	36	17
46.7	0·890	0·41	9·09	9	10
56.2	0·570	39·96	−16·22	43	28
56.5	0·755	−12·26	59·50	61	76
66.0	0·575	57·89	0	58	63
66.3	0·660	17·09	5·16	18	*w*
66.6	0·865	17·46	9·86	20	24
76.1	0·635	15·14	8·46	17	14
76.4	0·760	10·28	0·64	10	22
76.7	0·975	− 0·19	−13·93	14	10
86.2	0·710	−28·15	− 6·29	29	32
86.5	0·860	7·51	− 3·63	8	14
96.0	0·725	40·95	−16·30	44	20
96.3	0·795	− 3·65	−19·60	20	30
96.6	0·970	16·20	1·53	16	*w*
10.6..4	0·890	31·91	−47·76	58	55
11.6..2	0·855	−12·50	− 5·65	14	*w*
12.6..0	0·880	− 1·91	19·33	19	0
12.6..3	0·940	− 9·22	−23·42	25	28
13.6..1	0·940	15·22	10·72	19	17
07.2	0·445	−53·95	− 2·69	54	20
07.5	0·660	2·35	0·14	2	0
07.8	0·940	−12·08	−17·35	21	*w*
17.3	0·530	21·10	−37·61	43	35
17.6	0·770	0·39	32·43	32	24
27.1	0·465	49·60	5·01	50	80
27.4	0·625	−24·69	− 6·82	25	10
27.7	0·875	12·36	− 0·41	12	10
37.2	0·540	−14·10	−10·21	17	10
37.5	0·730	2·23	18·04	18	10
47.3	0·625	−15·11	−16·01	22	14
47.6	0·835	17·72	2·23	18	*w*
57.1	0·590	27·45	19·48	34	20
57.4	0·720	− 8·00	−20·12	22	10
57.7	0·950	14·00	8·95	17	14
67.2	0·660	9·74	− 1·53	10	*w*
67.5	0·825	24·95	− 0·06	25	14
77.0	0·675	−22·97	0	23	*w*
77.3	0·745	9·70	− 8·38	13	28
77.6	0·930	−25·44	13·94	29	32
87.1	0·730	4·04	31·98	32	10
87.4	0·840	−11·92	−17·63	21	20
97.2	0·800	28·55	4·38	29	14
97.5	0·940	−16·80	− 2·49	17	14

Reflection	sin θ	$A_{calc.}$	$B_{calc.}$	$\lvert F_{calc.}\rvert$	$F_{obs.}$
10.7..0	0·820	− 6·99	− 1·06	7	*w*
10.7..3	0·885	1·88	− 3·09	4	14
11.7..1	0·880	1·79	8·53	9	14
11.7..4	0·970	− 1·95	− 3·48	4	0
12.7..2	0·950	−16·46	7·35	18	17
08.1	0·455	11·63	20·16	23	*w*
08.4	0·620	6·56	24·47	25	*w*
08.7	0·870	−26·87	− 4·34	27	26
18.2	0·520	− 7·99	33·22	34	22
18.5	0·715	5·71	−21·20	22	10
28.3	0·600	− 7·59	−34·51	35	33
28.6	0·820	− 6·52	26·06	27	24
38.1	0·560	9·88	− 1·32	10	20
38.4	0·695	−18·48	− 1·04	19	10
38.7	0·930	0·25	−15·20	15	17
48.2	0·625	−44·35	11·02	45	35
48.5	0·795	21·49	−31·81	38	22
58.3	0·710	3·00	13·00	13	20
58.6	0·900	−12·35	17·92	22	*w*
68.1	0·685	1·10	− 4·05	4	14
68.4	0·800	−12·06	8·52	15	30
78.2	0·755	−18·69	13·79	23	17
78.5	0·900	17·71	−16·07	24	20
88.0	0·770	−10·42	0	10	17
88.3	0·835	8·10	− 4·38	9	22
98.1	0·825	26·85	− 5·48	28	22
98.4	0·925	−19·46	16·31	25	14
10.8..2	0·895	−17·45	− 0·38	17	10
11.8..0	0·920	− 8·66	0·27	9	17
11.8..3	0·970	7·66	−16·85	19	10
09.3	0·595	20·14	23·52	31	10
09.6	0·815	−25·84	− 5·57	26	28
19.1	0·540	− 8·57	10·60	14	24
19.4	0·680	15·90	−31·23	35	22
19.7	0·920	− 9·07	5·07	10	*w*
29.2	0·605	1·46	−12·89	13	*w*
29.5	0·780	6·20	− 1·80	6	20
39.3	0·680	24·93	0·98	25	14
39.6	0·880	−29·44	−19·15	35	14
49.1	0·650	− 1·06	9·16	9	14
49.4	0·770	17·59	7·74	19	22
59.2	0·715	−26·69	− 2·80	27	20
59.5	0·870	22·51	26·78	35	24
69.3	0·795	− 0·39	26·95	27	28
79.1	0·780	−24·46	7·37	26	24
79.4	0·880	40·52	− 8·89	41	20
89.2	0·845	−24·13	0·85	24	17
99.0	0·865	32·66	0	33	10
99.3	0·925	−20·31	− 7·48	22	26
10.9..1	0·920	0·04	1·64	2	10
0.10..2	0·595	29·53	16·39	34	30
0.10..5	0·770	−51·25	38·04	64	41
1.10..3	0·670	−17·79	−16·45	24	*w*
1.10..6	0·870	16·71	11·47	20	20
2.10..1	0·630	12·73	16·15	21	22
2.10..4	0·750	− 5·49	−21·45	22	10
3.10..2	0·690	−25·09	29·99	39	14
3.10..5	0·845	14·20	−10·54	18	32
4.10..3	0·765	3·88	− 1·96	4	10
4.10..6	0·945	5·54	3·82	7	*w*
5.10..1	0·740	−34·53	1·41	35	33
5.10..4	0·850	32·86	−23·08	40	32
6.10..2	0·805	18·19	26·34	28	24
6.10..5	0·945	−19·96	12·36	24	26
7.10..3	0·885	−14·64	− 4·19	15	14
8.10..1	0·875	21·82	− 3·21	22	17
8.10..4	0·970	− 2·94	6·23	7	10
9.10..2	0·940	− 1·98	− 6·51	7	10
10.10..0	0·960	40·13	0	40	40
0.11..1	0·620	−56·62	8·10	57	67
0.11..4	0·745	14·35	−60·61	62	70
0.11..7	0·970	−19·47	21·82	29	20

Table 3. (*cont.*)

Reflection	sin θ	$A_{calc.}$	$B_{calc.}$	$\lvert F_{calc.}\rvert$	$F_{obs.}$
1.11..2	0·675	12·49	−18·97	23	14
1.11..5	0·835	−12·01	− 3·79	13	17
2.11..3	0·745	2·76	−12·53	13	17
2.11..6	0·930	− 5·35	25·80	27	22
3.11..1	0·715	18·95	15·60	25	20
3.11..4	0·830	− 8·82	5·64	10	*w*
4.11..2	0·780	− 2·23	17·00	17	20
5.11..3	0·850	−20·82	19·74	29	22
6.11..1	0·835	−29·71	5·72	30	24
6.11..4	0·935	1·04	−12·33	12	32
7.11..2	0·900	−10·00	14·36	17	10
8.11..3	0·970	11·73	− 6·37	13	*w*
9.11..1	0·970	−14·21	− 1·95	14	10
0.12..3	0·740	− 0·51	4·21	4	*w*
0.12..6	0·925	−14·07	−25·69	29	14
1.12..1	0·705	1·00	− 4·15	4	*w*
1.12..4	0·815	5·93	2·51	6	*w*
2.12..2	0·760	−19·12	− 7·24	21	22
2.12..5	0·905	25·80	7·01	27	*w*
3.12..3	0·830	12·34	8·63	15	*w*
4.12..1	0·810	−35·04	− 0·90	35	24
4.12..4	0·910	25·51	− 4·89	26	39
5.12..2	0·870	−22·10	6·16	23	*w*
6.12..3	0·940	−19·63	2·11	20	17
7.12..1	0·930	10·32	13·76	17	14
0.13..2	0·755	−22·27	22·74	32	20
0.13..5	0·900	2·51	− 0·67	3	24
1.13..3	0·815	−18·25	−22·33	29	14
2.13..1	0·790	18·27	−10·45	21	20
2.13..4	0·895	− 8·02	18·88	21	22
3.13..2	0·845	−21·18	22·15	31	30
4.13..3	0·915	2·02	−18·95	19	14
5.13..1	0·900	21·56	3·77	22	10
6.13..2	0·960	−14·01	8·90	17	24
0.14..1	0·785	12·95	1·36	13	17
0.14..4	0·890	− 5·94	−30·61	31	17
1.14..2	0·835	0·43	−15·27	15	10
1.14..5	0·970	−13·91	16·52	22	17
2.14..3	0·900	− 5·44	− 1·16	6	10
3.14..1	0·880	30·30	23·08	38	20
3.14..4	0·970	− 9·99	− 4·71	11	*w*
4.14..2	0·935	7·98	7·37	11	10
0.15..3	0·895	−23·69	0·76	24	*w*
1.15..1	0·870	−30·22	−15·68	34	17
1.15..4	0·965	12·56	−15·67	20	30
2.15..2	0·920	− 7·75	−10·73	13	14
4.15..1	0·970	−14·47	8·20	17	14
0.16..2	0·915	1·12	3·51	4	*w*
1.16..3	0·970	− 7·35	7·11	10	10
2.16..1	0·955	11·04	1·45	11	14

Remark: 21.21..0 was observed as a strong reflection on a film exposed to Mo$K\alpha$ radiation.

Maximum possible value for $F_{21.21..0}=63$, $F_{calc.}=45$.

International Union of Crystallography

Report of Executive Committee for 1949

Introduction

During 1949 the Union was engaged in carrying out the programme of activities initiated at the First General Assembly at Harvard University in 1948, and in making preliminary arrangements for the Second General Assembly to be held at Stockholm in 1951. The majority of these activities were conducted under the auspices of the several Commissions and are reported in detail below. The number of Adhering Bodies increased to eleven, and four other countries gave notice of adhesion as from 1 January 1950. Details of these fifteen countries are given in Table 1.

Table 1. *Adhering Bodies*

Country	Group*	Secretary of National Committee
Australia	I	R. I. Garrod, Defence Research Laboratories, Private Bag No. 4, P.O. Ascot Vale W. 2, Victoria
Belgium	III	R. Van Tassel, Conservateur au Musée d'Histoire Naturelle, Brussels
Canada	IV	W. H. Barnes, Division of Physics, National Research Council, Ottawa
Czechoslovakia	I	The Secretary, Czechoslovak National Research Council, Opletalova 19, Prague II
Denmark	I	A. Tovborg Jensen, Den Kgl. Veterinær- og Landbohøjskoles kemiske Laboratorium, Copenhagen 5
France	VII	V. Luzzati, Laboratoire Central des Services Chimiques de l'État, 12 quai Henri IV, Paris 4
India	I	The Secretary to the Government of India, Department of Scientific Research, North Block, Central Secretariat, New Delhi
Japan	I	T. Ito, National Committee for Crystallography, Science Council of Japan, Ueno Park, Tokyo
Netherlands	IV	E. H. Wiebenga, Bloemsingel 10, Groningen
Norway	I	I. Oftedal, Mineralogisk Institutt, Blindern, Oslo
South Africa	I	The Officer-in-Charge, Liaison Division, South African Council for Scientific and Industrial Research, P.O. Box 395, Pretoria
Spain	IV	M. A. Berger, Instituto 'Alonso de Santa Cruz', Serrano 119, Madrid
Switzerland	I	M. Vuagnat, Muséum d'Histoire Naturelle, Geneva
United Kingdom	VIII	The Secretary of the British National Committee for Crystallography, The Royal Society, Burlington House, London W. 1
United States of America	VIII	R. W. G. Wyckoff, Laboratory of Physical Biology, National Institute of Health, Bethesda 14, Maryland

* See Statutes 8 and 10 (*Acta Cryst.* (1948), **1**, 275).